Helium Induced Structural Disorder in Hydrogenated Nanocrystalline Silicon (nc-Si:H) Thin Films Prepared by HW-CVD Method

Nabeel A. Bakr*

Department of Physics, College of Science, University of Diyala, Diyala - Iraq

Structural, optical and electrical properties of hydrogenated nanocrystalline silicon (nc-Si:H) films, deposited from silane (SiH_4) and helium (He) gas mixture without hydrogen by hot wire chemical vapor deposition (HW-CVD) method were investigated as a function of helium dilution of silane (R_{He}). We observed that the deposition rate is much higher (4-33 Å/s) compared to conventional plasma enhanced chemical vapour deposited (PE-CVD) nc-Si:H films. Raman spectroscopy revealed that the crystalline volume fraction decreases with increasing He dilution of silane whereas the crystallite size remains almost constant (~ 2 nm) for the entire range of He dilution of silane studied. Furthermore, an increase in the structural disorder in the nc-Si:H films has been observed with increasing He dilution of silane. The hydrogen content was ~ 9 at. % in the film deposited at 60 % R_{He} and decreases rapidly as R_{He} increases further. The photoresponse decreases by order of 1 with increasing helium dilution of silane from 60 to 97 %. It has been concluded that adding helium gas to the silane induces the structural disorders in the hydrogenated nanocrystalline silicon (nc-Si:H) thin films prepared by HW-CVD method.
.

Keywords: HW-CVD, Hydrogenated Nanocrystalline Silicon, Helium Dilution of Silane, Raman Spectroscopy, Structural Disorder.

PACS numbers: 81.15.Gh, 81.07.Bc, 73.63.Bd

1. INTRODUCTION

Hydrogenated nanocrystalline silicon (nc-Si:H) is a structurally inhomogeneous material which consists of nanometer-size Si crystallites embedded in an amorphous tissue, along with grain boundaries (GBs) and microvoids [1, 2]. Such material exhibits a variety of microstructures and physical properties that depend strongly on the preparation conditions. These materials show interesting properties such as high conductivity, high charge carrier mobility and high doping efficiency [3-5], thus they have attracted a great deal of attention in recent years in many potential applications such as third generation solar cells [6, 7], photodiodes [8] and thin film transistors [4]. Although high hydrogen dilution facilitates the microcrystallization of silicon films, it also reduces the deposition rate drastically which is a serious barrier towards achieving reasonably cost-effective throughput in large-scale commercial production of optoelectronic devices. However, in preparation of nc-Si:H films by conventional PE-CVD method, dilution of silane (SiH_4) with noble gasses, high deposition rates can be achieved at a low level of electrical excitation. The dilution of silane with Argon (Ar), Helium (He), or Xenon (Xe) has a strong influence on the structure and morphology of the films. For example, it has been reported that addition of Ar in SiH_4 plasma introduces rapid crystallization of a-Si:H network. However, extremely high Ar dilution adversely affects the nanocrystallization process and induces the growth of columnar structures [8]. A number of efforts have been made towards preparation of nc-Si:H films from SiH_4 plasma using He dilution. In some cases it is either, amorphous [9], polymorphous [10], microcrystalline [11] or nanocrystalline network [12]. Xe-dilution normally maintains an amorphous nature of the network even at a very high power applied to silane plasma [13]. It has been identified that hydrogen dilution of silane is not an essential condition for the formation of nanocrystalline silicon [14] and the inert gases dilution of silane is another way to produce nc-Si:H thin films. K. Bhattacharya and D. Das [15] have studied the effect of rf power on the nanocrystallization of a-Si:H network by PE-CVD at a substrate temperature of 200 °C and a gas pressure of 0.5 Torr using silane as the source gas and helium as diluent, without using hydrogen. They have shown that the structural transformation from amorphous to nanocrystalline phase accomplished by metastable helium atoms in the plasma was identified at low rf power of 80 W. With an increase in the applied rf power up to 150 W, systematic improvement in crystallinity has been achieved with crystalline volume fraction of ~ 77 % and grain size of ~ 7 nm. The deposited films showed reduced bonded hydrogen content (~ 8 %), enhanced polymerization in the network and gradual widening in the optical bandgap (~ 1.86 eV) obtained at a high deposition rate (107 Å/min) using 1 sccm of silane as the source gas and 69 sccm of helium as the only diluent. Raha and Das [16] have studied the effect of partial hydrogen dilution on the mostly helium diluted silane plasma in controlling the nanocrystallization process in the Si:H network. The parametric conditions were chosen in such a way as to produce the basic matrix as a mixed phase heterogeneous material in the neighborhood of amorphous to nanocrystalline transition zone, but dominated by the amorphous component, which could easily trigger nanocrystallization on favorable parametric changes. They have shown that the energy released by de-excitation of

---

* nabeelalibakr@yahoo.com

He* is utilized in breaking up strained and weak Si-Si bonds and remaking strong Si-Si bonds at the boundary of c-Si nucleation centers and the amorphous matrix thereby creating a more relaxed and compact network structure. They have demonstrated that the inclusion of a small amount of H_2 as a component diluent introduces a radical change in the material properties and that continued at higher partial H_2-dilution relative to that of He in the plasma. The optical absorption was reduced; the optical band gap was widened and sharp reduction in the bonded hydrogen content was observed. The overall crystallinity in the material increased sharply, the porosity in the material reduced grossly and the electrical conductivity increased by several orders of magnitude. All this happened at the cost of a relatively insignificant lowering in the growth rate of the material because of the trivial amount of the required H_2-dilution. In this study, the detailed investigation of structural, optical and electrical properties of nc-Si:H films deposited by HW-CVD as a function of He dilution of SiH_4 without hydrogen is presented. The synthesis of nc-Si:H thin films using PE-CVD method has been extensively studied in the past. However, to the best our knowledge up to now the HW-CVD method has not been studied for the synthesis of nc-Si:H films using noble/inert gas dilution of SiH_4 and no reports exist in the literature. With this motivation, we initiate the study of synthesis and characterization of nc-Si:H films with He dilution of SiH_4 by using HW-CVD method. We believe that the addition of noble gases diluents will change the nature of the deposition mechanism from CVD-like to PVD-like process. Thus, the detailed knowledge of the structural, optical and electrical properties of nc-Si:H thin films deposited under a wide range of deposition conditions including the noble gases dilution of silane, is of great importance from the viewpoints of both fundamental physics and technological future applications.

2. EXPERIMENTAL DETAILS

2.1 Film preparation

Intrinsic hydrogenated nanocrystalline silicon (nc-Si:H) thin films were deposited simultaneously on Corning #7059 glass and c-Si wafers (311) in a HW-CVD system, details of which have been described elsewhere [17]. Films were prepared by using a mixture of pure SiH_4 (Matheson Semiconductor Grade) and He (Ultra High Pure) gases. The helium flow rate was kept constant (30 sccm) while SiH_4 flow rate was varied from 1 sccm to 20 sccm. The temperature of the tungsten filament was maintained at 1900 ± 5 °C due to reason mentioned elsewhere[18]. Substrate temperature was held constant during the deposition at the desired value accurately using a thermocouple and temperature controller. Other deposition parameters are listed in Table 1.

The glass substrates were initially washed by soap solution and rinsed well in distilled water followed by cleaning in ultrasonic bath for 5 minutes. Then four stages of substrates cleaning were done: i) Placing the substrates in acetone bath for 5 minutes, ii) Placing the substrates in methanol bath for 5 minutes, iii) Placing

the substrates in dilute hydrochloric acid (30 %) bath for 30 minutes and, iv) Placing the substrates in dilute nitric acid (30 %) bath for 30 minutes [19], before rinsing them again in distilled water and flushed them with nitrogen. The c-Si wafers were cleaned by a 1 minute dip in dilute HF (5 %) to remove the native oxide layer from the wafer surface [20].

Table 1 – Deposition parameters for deposition of intrinsic nc-Si:H films

Deposition Parameter	Value
Filament temperature (T_{fil})	1900 ± 5 °C
Deposition pressure (P_{dep})	50 mTorr
Substrate temperature (T_{sub})	450 ± 5 °C
He dilution of SiH_4 $R_{He} = F_{He}/(F_{He} + F_{SiH4})$	60-97 %
Filament to substrate distance ($d_{s\text{-}f}$)	2.75 cm
Deposition time (t)	10-60 min

The above cleaning method provides good adhesion of the films to the substrates. The substrates were loaded and the deposition chamber was evacuated to a base pressure less than 10^{-6} mbar. The chamber was baked for 4-5 hours at a temperature of 200 °C prior to each deposition to minimize the possibility of the contamination of the deposited films. Then the substrate was heated to the desired temperature by setting the temperature controller. The chamber then was purged by hydrogen before introducing pure SiH_4 gas (Matheson Semiconductor Grade) and He gas (Ultra High Pure) inside the chamber and starting the deposition process. The deposition was carried out for the desired amount of time and the films were allowed to cool down to room temperature in vacuum. It is worthy to indicate that using the deposition parameters stated in the literature didn't produce the same structure of the resultant films. This has led to the conclusion that the deposition parameters are system dependent [21-23].

2.2 Film characterization

The dark conductivity (σ_{dark}) and photoconductivity (σ_{photo}) were measured with coplanar Al electrodes. Fourier transform infrared (FTIR) spectra of the films were recorded by using FTIR spectrophotometer (Shimadzu, Japan). Bonded hydrogen content (C_H) was calculated from wagging mode of IR absorption peak using the method given by Brodsky et al. [24]. The band gap was estimated using the procedure followed by Tauc [25]. Raman spectra were recorded with micro-Raman spectroscopy (Jobin Yvon Horibra LABRAM-HR) in the wavelength range of 400-700 nm. The spectrometer has backscattering geometry for detection of Raman spectrum with the resolution of 1 cm^{-1}. The excitation source was 632.8 nm line of He-Ne laser. The power of the Raman laser was kept less than 5 mW to avoid laser induced crystallization on the films. The Raman spectra were deconvoluted in the range of 400-540 cm^{-1} using Levenberg-Marquardt method [26]. The crystalline fraction (X_{Raman}) was then deduced using the meth-

od proposed by Kaneko et al. [27]. The crystallite size (d_{Raman}) was calculated from:

$$d_{Raman} = 2\pi \sqrt{\left(\frac{\beta}{\Delta\omega}\right)}$$

where $\Delta\omega$ is the peak shift for the hydrogenated nano-crystalline silicon (nc-Si:H) compared to the crystalline silicon (c-Si), and $\beta = 2.0$ nm^2 cm^{-1} [28]. Low angle x-ray diffraction spectra were obtained by x-ray diffractometer (Bruker D8 Advance, Germany) using Cu K$_\alpha$ line ($\lambda = 1.54056$ Å). The spectra were taken at a grazing angle of 1°. The average crystallite size was estimated using the classical Scherrer's formula:

$$d_{x-ray} = \frac{0.9\,\lambda}{B\cos\theta_B}$$

The thickness of films was measured by a Talystep profilometer (Taylor-Hobson Rank).

3. RESULTS AND DISCUSSION

3.1 Variation of deposition rate

The variation of deposition rate (r_d) as a function of He dilution of silane (R_{He}) is shown in Figure 1. As seen from the figure, the deposition rate decreases from ~ 33 Å/s to ~ 3.9 Å/s with increasing Helium dilution of silane from 60 % to 97 %.

The decrease in deposition rate with increasing He dilution of silane can be attributed to the decrease in the SiH$_4$ density in the gas mixture. As a result, the concentration of precursors that produce Si:H film decreases and consequently, the deposition rate decreases with increasing He dilution of silane. The decrease in the deposition rate with increasing He dilution of silane was reported previously for PE-CVD deposited nanocrystalline and polymorphous Si:H films [29, 30]. It is interesting to note that under the same deposition conditions the observed deposition rate is significantly higher than that of hydrogen dilution of silane [31] and argon dilution of silane [32]. This can be attributed to the non-etching properties of He [33].
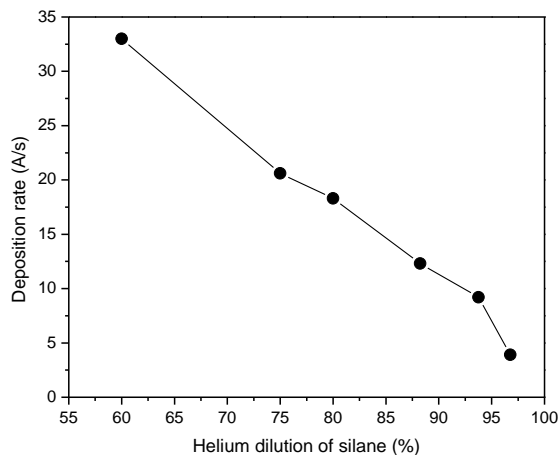
Fig. 1 – Variation of deposition rate as function of He dilution of silane

3.2 Micro-Raman spectroscopic analysis

Figure 2 shows Raman spectra of nc-Si:H films deposited at various helium dilution of silane (R_{He}). The following observations have been made from the Raman spectra for the films deposited at different He dilution of silane:
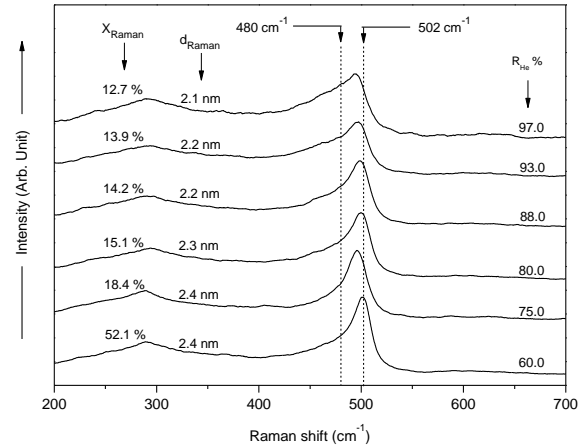
**Fig. 2** – Raman spectra of nc-Si:H films deposited by HW-CVD at various He dilution of silane

1) Raman spectra of all films consist of two peaks; one is centred at 480 cm^{-1} corresponding to the TO$_1$ band of the amorphous phase and the other centred between 500 cm^{-1} and 502 cm^{-1} corresponding to the TO$_2$ band of crystalline phase present in the material. With increase in He dilution of silane, a slight change in the shape and intensity of TO peak has been observed. The TO$_2$ peak is slightly shifted towards lower wave number which indicates a mild change in crystallite size in the film.

2) The crystalline volume fraction (X_{Raman}) decreases from ~ 52 % to ~ 13 % as the helium dilution of silane increases from 60 % to ~ 97 % while the crystallite size (d_{Raman}) remains in the range of 2.4 – 2.1 nm for the entire range of helium dilution of silane studied. The abrupt drop in the crystalline volume fraction from 52 % for the film deposited at 60 % of He dilution of silane to 18 % for the film deposited at 75 % He dilution of silane indicates the nanocrystalline-to-amorphous transition in the film.

3) The variation of full width at half maximum of the peak T$_{O1}$ (Γ_{TO1}) is a measure of bond angle deviation ($\Delta\theta$) in the amorphous network and taken as a measure of the disorder in the film [34]. Figure 3 shows the variation of ($\Delta\theta$) as a function of helium dilution of silane. It can be seen from the figure that ($\Delta\theta$) increases from 6.4° to 8.2° as the helium dilution of silane increases from 60 % to 97 % This result indicates that with increasing He dilution of silane, the structural disorders in the film also increases.

It is reported that the use of He dilution of silane in PE-CVD process is beneficial in enhancing the growth rate and initiating the nanocrystallization within the heterogeneous structure [35]. Bahattacharya and Das [36] proposed that with helium as a diluent gas, a large amount of energy happens to be transferred to the growth zone by the bombardment of ionized He$^+$ ions and metastable He* atoms from the plasma. This energy

breaks up the weak Si-Si bonds and a portion of it may also be utilized in releasing the loosely bonded hydrogen from SiH$_2$ sites.
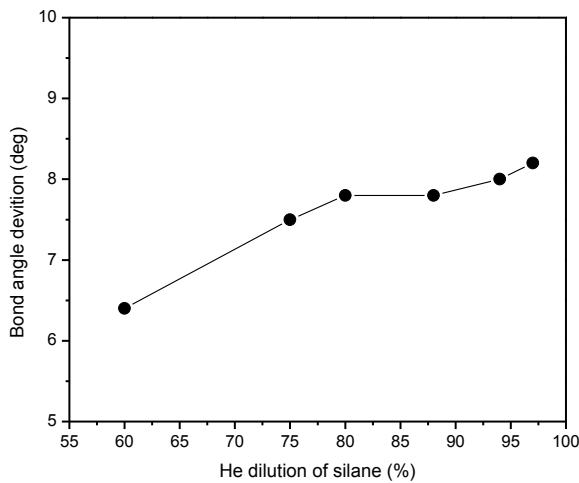

Fig. 3 – Bond angle deviation ($\Delta\theta$) of nc-Si:H films deposited by HW-CVD as a function of He dilution of silane

The dangling bonds produced by breaking the weak Si-Si bonds, form strong bonds with silicon or are terminated by hydrogen. By this process the strain at the boundary of crystalline Si nucleation centres and amorphous matrix will get relaxed. However, it seems that the above assumption is not valid in HW-CVD process since the hot filament source cannot ionize the helium gas because of its high ionization energy (24.6 eV) and the number of excited helium atoms is relatively small due to the high excitation energy (19.85 eV). Therefore, we believe that the addition of helium gas in HW-CVD chamber mainly has a dilution effect on the reactant species. As a result, the radicals and atomic H may have a greater lifetime (or a larger mean free path) which increases their concentration at the substrate surface [37]. This conjecture is well supported by the enhanced growth rate obtained in this study (see Figure 1). We assume that the energy required for the formation of nano crystals in the amorphous network (Gibb's free energy for crystallization) is not available in the growth zone using He dilution of silane. This is mainly due to the low mass of He (Helium is ten times lighter than Argon) which results in inefficient thermal energy transfer to the growing surface. Thus, we conclude that the addition of He to the HW-CVD chamber without using hydrogen is not beneficial and has a deteriorating effect on the structural properties of the deposited material.

3.3 Low angle x-ray analysis

The X-ray diffraction patterns of nc-Si:H films deposited on c-Si at different helium dilution of silane (R_{He}) are shown in Figure 4. The only feature observed for all films is a broad peak occurring at $2\theta = 27°$ corresponding to (111) crystal orientation and less intense peaks occur at $2\theta \sim 41°$ and $2\theta \sim 53°$ corresponding to (200) and (311) crystal orientations.

The dominant peak is (111). This result indicates that the crystallites in nc-Si:H films have preferential orientation in (111) direction. As seen from the spectra
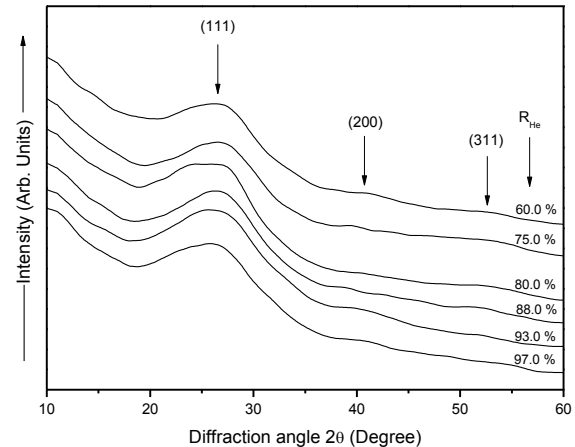
Fig. 4 – XRD patterns of some nc-Si:H films deposited at different He dilution of silane

a shift in (111) diffraction peak to a lower angle is observed with increasing helium of silane suggesting the increase in the compressive stress of the films [38]. The average crystallite size (d_{x-ray}) for all films is ~ 2 nm and this agrees well with the results obtained from Raman analysis.

3.4 Fourier transform infrared (FTIR)

The FTIR spectra (normalized for thickness) of nc-Si:H films deposited by HW-CVD at different helium dilution of silane (R_{He}) are shown in Figure 5. It is clear that the films deposited at $R_{He} \leq 88$ % have three major absorption bands at ~ 638 cm^{-1}, ~ 1990 cm^{-1} and 2085 cm^{-1} corresponding to the wagging vibrational modes of different bonding configurations, the stretching vibrational mode of mono-hydrogen (Si-H) bonded species and the stretching vibrational modes of di-hydrogen species (SiH$_2$) and (Si-H$_2$)$_n$ complexes (isolated or coupled) respectively [39-41]. It is clearly seen that the absorption band at 1990 cm^{-1} almost vanishes for the films deposited at $R_{He} \geq 93$ %. Thus, for the films deposited at high R_{He}, the bonded hydrogen is incorporated mainly in di-hydrogen species (SiH$_2$) and (Si-H$_2$)$_n$ complexes. These features indicate that the predominant hydrogen bonding in HW-CVD deposited nc-Si:H films shifts from Si-H$_2$ and (Si-H$_2$)$_n$ complexes to Si-H with decrease in helium dilution of silane. The microstructure parameter (R^*) is determined by using:

$$R^* = I_{2085}/(I_{2085} + I_{1990})$$

Where I_{1990} and I_{2085} are the integrated absorption intensities at 1990 cm^{-1} and 2085 cm^{-1}, respectively.

Figure 6(a) shows the variation of microstructure parameter (R^*) as a function of He dilution of silane (R_{He}). It is clearly seen that R^* increases with increase in R_{He} indicating the deterioration of the film quality with increase in helium dilution of silane.

These results are in agreement with the results obtained from Raman spectroscopy analysis. Figure 6(b) shows the estimated bonded hydrogen content (C_H) in nc-Si:H films as a function of helium dilution of silane (R_{He}). It can be clearly seen that the hydrogen content decreases from ~ 9 at. % to ~ 3.7 at. % as R_{He} increases from 60 % to 97 %. The high hydrogen content
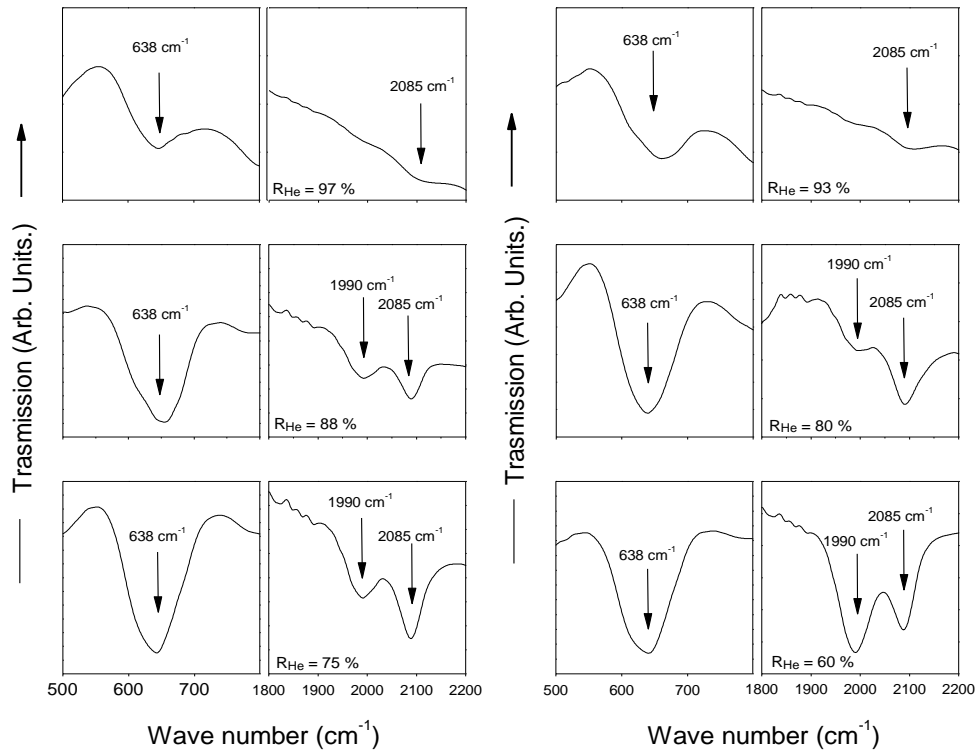
Fig. 5 – FTIR spectra of nc-Si:H films at different He dilution of silane. (For clarity, the spectra have been split horizontally into two parts)
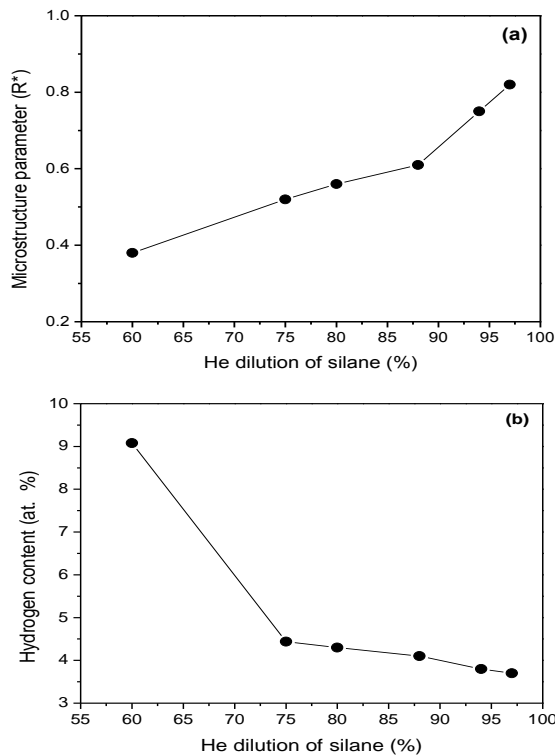

Fig. 6 – Variation of **(a)** Microstructure parameter and **(b)** Hydrogen content of nc-Si:H films deposited by HW-CVD as a function of He dilution of silane

($\sim$ 9 at. %) in the film deposited at 60 % R_{He} may be due to high crystalline volume fraction ($\sim$ 52 %) in the film. The high crystalline volume fraction with small crystallite size ($\sim$ 2 nm) suggests the formation of an increasing number of nanocrystalline grains in the amorphous network and hence a large number of grain boundaries [15]. This increases total surface area of grains which act as reservoirs of hydrogen in the material [42]. In fact, the dense hydrogen atoms which are concentrated at the grain boundaries limit the further growth of small crystallites [43] and result in almost constant crystallite size for the entire range of He dilution of silane studied.
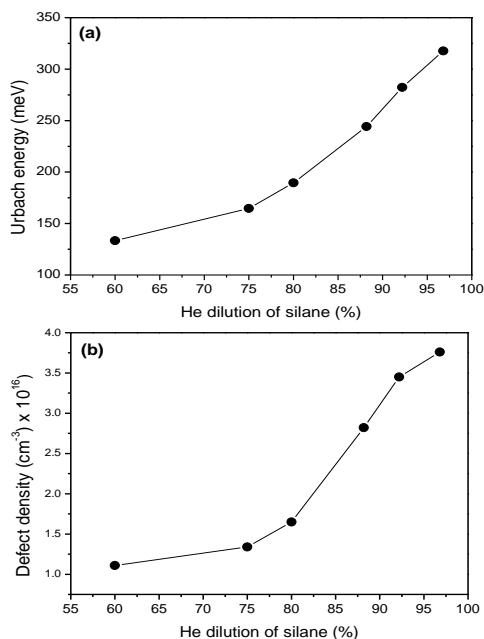
3.5 Optical properties

Figure 7 shows the variation of the band gap (E_g) as a function of He dilution of silane (R_{He}) for the nc-Si:H thin films deposited by HW-CVD. It can be seen that with the increase in He dilution of silane from 60 % to 97 % the band gap decreases from 1.66 eV to 1.54 eV. The decrease in the band gap may be due to the decrease in hydrogen content in the films (see Figure 6).

Figure 8 shows the Variation of Urbach energy and defect density as a function of helium dilution of silane. The Urbach energy (E_o) of the deposited films increases from 138 to 318 meV and the defect density (N_d) increases from $\sim 1 \times 10^{16}$ to $\sim 3.8 \times 10^{16}$ cm^{-3} as R_{He} increases from 60 % to 97 %. The typical value of the defect density for device quality a-Si:H films is $< 1 \times 10^{16}$ cm^{-3} [40]. These results again indicate that the properties of the deposited films degrade with increasing the helium dilution of silane in HW-CVD.
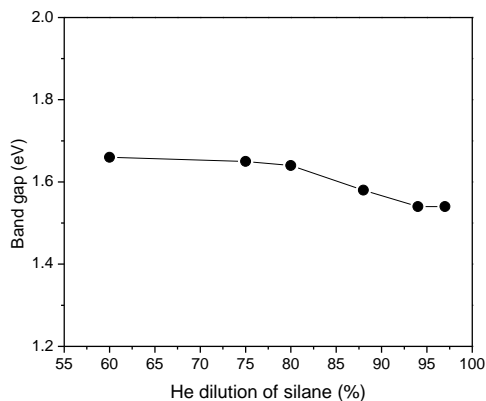
**Fig. 7** – Variation of band gap as a function of helium dilution of silane

Fig. 8 – Variation of (a)Urbach energy and (b)defect density as a function of helium dilution of silane

3.6 Electrical properties

The effect of helium dilution of silane (R_{He}) on dark conductivity (σ_{Dark}) and photoconductivity (σ_{Photo}) of nc-Si:H films is shown in Figure 9. As seen from the figure, there is a slight increase in σ_{Dark} in the range of $\sim 10^{-7}$ S/cm when helium dilution of silane increase from 60 % to 80 % and then decreases to $\sim 10^{-8}$ S/cm as the helium dilution of silane increases further to 97 %, whereas the σ_{Photo} remains almost constant in the range 10^{-4} S/cm as the helium dilution of silane increases from 60 to 80 % and then decreases to 10^{-6} S/cm as the helium dilution of silane increases further to 97 %.

As a result, photoresponse ($\sigma_{Photo} / \sigma_{Dark}$) decreases from $\sim 2.7 \times 10^3$ to 2×10^2 when the helium dilution of silane increases from 60 % to 97 %. These results support the deterioration effect of helium dilution of silane on the structural as well as the optical properties of nc-Si:H films deposited films by HW-CVD.
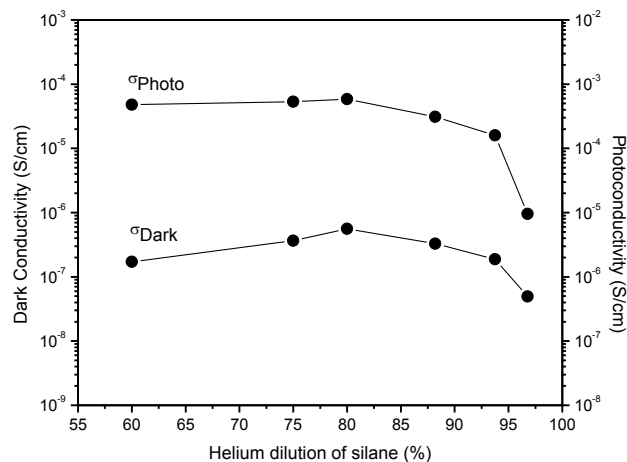
Fig. 9 – Variation in dark and photoconductivity of nc-Si:H films as a function of He dilution of silane

4. CONCLUSION

Intrinsic hydrogenated nanocrystalline silicon (nc-Si:H) thin films have been deposited by HW-CVD technique using SiH_4 as a source gas and He as a dilution gas. The effect of He dilution of silane on structural, optical and electrical properties has been studied in detail. The deposition rate decreases with increase in He dilution of silane and it was found that it is higher than that of Ar and H_2 diluted films under the same process parameters. From Raman spectroscopic analysis it has been found that the crystalline volume fraction decreases with increasing He dilution of silane whereas the crystallite size remains almost constant (~ 2 nm) for the entire range of He dilution of silane studied. Furthermore, an increase in the structural disorder in the nc-Si:H films has been observed with increasing He dilution of silane. FTIR analysis clearly indicates that with increasing He dilution of silane the hydrogen bonding shifts from Si-H bonding to Si-H_2 species and (Si-H_2)$_n$ complexes configuration. The hydrogen content was ~ 9 at. % for the film deposited at 60 % R_{He} and decreases rapidly as R_{He} increases further. The structure parameter (R^*) has an increasing trend against He dilution of silane suggesting the degradation of the quality of films. The band gap decreases with increasing He dilution of silane and it is attributed to the decrease in hydrogen content in the films. The photoresponse decreases by order of 1 with increasing He dilution of silane from 60 to 97 %. It has been concluded that He has deteriorating effect on the film properties and it induces the structural disorders in hydrogenated nanocrystalline silicon (nc-Si:H) thin films prepared by HW-CVD method.

REFERENCES

1. G. Yue, J.D. Lorentzen, J. Lin, Q. Wang, D. Han, *Appl. Phys. Lett.* **75**, 492 (1999).
2. G. Yue, D. Han, D. Willamson, J. Yang, K. Lord, S. Guha, *Appl. Phys. Lett.* **77**, 3185 (2000).
3. M. Ito, C. Koch, V. Svrcek, M. Schubert, J. Werner, *Thin Solid Films* **383**, 129 (2001).
4. C.-H. Lee, A. Sazonov, A. Nathan, *Appl. Phys. Lett.* **86**, 222106 (2005).
5. M. Jana, D. Das, A.K. Barua, *J. Appl. Phys.* **91**, 5442 (2002).
6. J. Yang, B. Yan, S. Guha, *Thin Solid Films* **487**, 162 (2005).
7. R.E. Schropp, H. Li, R. Franken, J. Rath, C. Van der Werf, J. Schuttauf, R. Stolk, *Thin Solid Films* **516**, 6818 (2008).
8. D. Das, M. Jana, A.K. Barua, *J. Appl. Phys.* **89**, 3041 (2001).
9. S.-W. Lee, D.-C. Heo, J.-K. Kang, Y.-B. Park, S.-W. Rhee, *J. Electrochem Soc.* **145**, 2900 (1998).
10. M.A. Fontcuberta, R. Brenot, E.A.G. Hamers, R. Vanderhaghen, P.R. Cabarrocas, *J. Non-Cryst. Solids* **266-269**, 48 (2000).
11. J. Carabe, J. Gandia, N. Gonzalez, M. Guitierrez, *Appl. Surf. Sci.* **75**, 492 (1999).
12. K. Bhattacharya, D. Das, *Bull. Mater. Sci.* **31/3**, 467 (2008).
13. A. Matsuda, S. Mashima, K. Hasezaki, A. Suzuki, S. Yamasaki, P.J. McElheny, *Appl. Phys. Lett.* **58**, 2494 (1991).
14. A. Matsuda, *J. Non-Cryst. Solids* **59-60**, 767 (1983)
15. K. Bhattacharya, D. Das, *Nanotechnology* **18**, 415704 (2007).
16. D. Raha, D. Das, *J. Phys. D: Appl. Phys.* **41**, 085303 (2008).
17. S.R. Jadkar, J.V. Sali, M.G. Takwale, D.V. Musale, S.T. Kshirsagar, *Solar Energy Materials and Solar Cells* **64**, 333 (2000).
18. R.E.I. Schropp, K.F. Feenstra, E.C. Molenbroke, H. Meiling, J.K. Rath, *Philos. Mag.: B* **76**, 309 (1997).
19. G. Shugar, J. Ballinger, *Chemical Technicians-Ready Reference Handbook*, (McGraw Hill: New York: 1996).
20. K.A. Reinhardt, W. Kern, *Handbook of Silicon Wafer Cleaning Technology*, *2nd Edition*, (William Andrew Inc.: Norwich NY USA: 2007).
21. E. Mohamed, *Ph. D. Thesis*, (Murdoch University: Western Australia: 2004).
22. A. Pant, T.W.F. Russell, M.C. Huff, *Ind. Eng. Chem. Res.* **40**, 1377 (2001).
23. E.C. Molenbroek, A.H. Mahan, *J. Appl. Phys.* **82**, 1909 (1997).
24. M.H. Brodsky, M. Cardona, J.J. Cuomo, *Phys. Rev. B* **16**, 3556 (1977).
25. J. Tauc, *Optical Properties of Solids*, *Edited by F. Abeles*, (North Holland: Amsterdam: 1972).
26. D.W. Marquardt, *J. Soc. Ind. Appl. Math.* **11**, 431 (1963).
27. T. Kaneko, M. Wakagi, K. Onisawa, T. Minemura, *Appl. Phys. Lett.* **64**, 1865 (1994).
28. Y. He, C. Yin, G. Cheng, L. Wang, X. Liu, G.Y. Hu, *J. Appl. Phys.* **75**, 797 (1994).
29. D.H. Levi, B.P. Nelson, E. Iwanizcko, C.W. Teplin, *Thin Solid Films* **455**, 679 (2004).
30. S. Tchakarov, D. Das, O. Saadane, A.V. Kharchenko, V. Suendo, F. Kail, P. Roca i Cabarrocas, *J. Non-Cryst. Solid* **338-340**, 668 (2004).
31. N.A. Bakr, A.M. Funde, K.D. Diwate, V.S. Waman, T.S. Salve, S.R. Jadkar, S.P. Gokhale, *Advanced Materials and their applications,* (*SCNAMA*), *Part* 2, 23-38 (Univ. of Technology: Baghdad: Iraq: 2009).
32. N.A. Bakr, A.M. Funde, V.S. Waman, M.M. Kamble, R.R. Hawaldar, D.P. Amalnerkar, V.G. Sathe, S.W. Gosavi, S.R. Jadkar, *Thin Solid Films* **519**, 3501 (2011).
33. A.R. Middya, S. Hazra, S. Ray, *J. Appl. Phys.* **76**, 7578 (1994).
34. D. Beeman, R. Tsu, M.F. Thorpe, *Phys. Rev. B* **32**, 874 (1985).
35. D. Raha, D. Das, *J. Phys. D: Appl. Phys.* **41**, 085303 (2008).
36. K. Bhattacharya, D. Das, *J. Phys. D.: Appl. Phys.* **41**, 155420 (2008).
37. G.F. Zhang, V. Buck, *Surf. Coat. Tech.* **160**, 14 (2002).
38. L. Sahu, N. Kale, N. Kulkarni, R. Pinto, R. Dusane, B. Schroder, *Thin Solid Films* **501**, 117 (2006).
39. W. Wei, G. Xub, J. Wang, T. Wang, *Vacuum* **81**, 656 (2007).
40. G. Lucovsky, *Sol. Cells* **2**, 431 (1980).
41. P. John, I.M. Odeh, M.J.K. Thomas, *Solid State Commun.* **41**, 341 (1982).
42. A.R. Middya, S. Hazra, S. Ray, *J. Appl. Phys.* **76/11**, 7578 (1994).
43. D. Han, J. Lorentzen, J. Weinberg-Wolf, L. McNeil, Q. Wang, *J. Appl. Phys.* **94**, 2930 (2003).